Hydrobiologia
DOI 10.1007/s10750-013-1498-5

PRIMARY RESEARCH PAPER

Inherent optical properties of suspended particulates in four temperate lakes: application of in situ spectroscopy

David Kalenak · Emmanuel Boss · Steven W. Effler

Received: 18 November 2012 / Revised: 8 March 2013 / Accepted: 23 March 2013

Abstract Instrumentation measuring hyperspectral particle attenuation and absorption was used to assess particle concentration and size, chlorophyll, and spectral characteristics as a function of depth in four temperate lakes of different trophy. Partitioning the absorption coefficient permitted us to analyze properties of phytoplankton absorption as a function of ambient illumination and hydrographic conditions. Stratification was found to be a controlling factor in the size distribution and concentration of particles. Bloom cycles (chlorophyll > 10 mg m^{-3}) were observed to evolve over several weeks but on occasion did change rapidly. Total chlorophyll concentration revealed the majority of the lakes did not follow the typical seasonal succession of biomass associated with temperate waters. Particle and chlorophyll concentration maxima did not always coincide, cautioning the use of chlorophyll *a* as a surrogate for algal biomass. Phytoplankton near the base of the euphotic zone, including a deep chlorophyll maximum in an oligotrophic system, were found to exhibit significant chromatic adaptation. Unique absorption peaks identified the ubiquitous presence of cyanobacteria in all four lakes. Finally, particle resuspension and possible nepheloid layers were observed in the two smallest lakes.

Keywords Suspended particulates · Optics · Phytoplankton absorption · Biogeochemistry

Handling editor: P. Nõges

D. Kalenak (✉) · E. Boss
School of Marine Sciences, University of Maine,
458 Aubert Hall, Orono, ME 04469, USA
e-mail: dskalena@syr.edu

S. W. Effler
Upstate Freshwater Institute, Syracuse, NY 13214, USA

Introduction

Suspended particulate matter is integral to many biogeochemical and physical (optical) processes that govern the trophic condition of a lake. It is a major source of organic matter and a principal factor determining the quantity and quality of solar energy penetrating the water column. By convention, any substance retained by a specific pore size filter (usually 0.2–0.4 μm) is considered an aquatic particle. Aquatic particles are routinely subdivided into fractions representing the biota (e.g., viruses, bacteria, and phytoplankton) along with various decomposition/metabolic byproducts (e.g., detritus and fecal pellets), and inorganic particulates such as lithogenic minerals (e.g., clay and quartz) and possibly biogenic-related material (e.g., calcite aggregates and silica frustules). Central to the productivity of a lake (as primary producers) are the phytoplankton, while other suspended particles are critical in the transport and fate of organic (e.g., nutrients and pollutants) and inorganic

Published online: 05 April 2013

(e.g., scavenging of trace elements) material throughout the water column (Eisma, 1993). Understanding how these particle-mediated processes affect lake ecology is still limited by temporal and spatial resolution of water sampling (Staehr et al., 2012) and our limited ability to measure rate processes.

While many algal species coexist in the same water body, phytoplankton have diverse physiological, and morphological characteristics and respond differently to a number of environmental factors such as vertical mixing, nutrient availability, and light modulation (Wetzel, 2001). As a result, phytoplankton populations often exhibit large variability in taxa and associated properties that can evolve over short-temporal scales (e.g., minutes to hours). For example, storm runoff can produce unpredictable variation in community assemblages with lag times spanning hours to days (Edson & Jones, 1988; Vanni et al., 2006), while strong turbulent mixing and internal wave induction has been shown to completely alter the community structure (Reynolds, 2002, and references therein). Variability in the mixing depth in stratified regimes also affects the sinking rate of the phytoplankton (Ptacnik et al., 2003), as well as nutrient and light availability (Diehl et al., 2002). Consequently, environmental forcings combined with other biotic factors (e.g., grazing), contribute to vertical patchiness in algal communities (Watson et al., 1997; Cullen & MacIntyre, 1998; see also Fogg, 1991). In addition, many of these interactions are likely to change due to the effects of climate change (Nõges et al., 2010). While the relative motility of phytoplankton and random physical events does insure discrete methods are statistically representative, sampling errors cannot be avoided (Lampert & Sommer, 2007; see also Marshall et al., 1988). It follows that when discrete measurements at fixed intervals in the pelagic zone are used to monitor lake water (e.g., Holdren et al., 2001) the estimate of integrated properties related to the biota, such as algal biomass, will likely be aliased because of insufficient sampling resolution.

In situ profiling at sub-meter resolution could address this problem. Here, we showcase the utility of in situ profiling instrument measuring the optical properties of suspended substances (along with hydrographic data) throughout the water column with high vertical resolution; surrogate methods help reveal changes in the bulk particle composition and concentration with depth, including those associated with phytoplankton, much of which would likely go undetected using discrete sampling.

Novel in situ profiling instruments capable of measuring hyperspectral absorption, $a(\lambda)$, and beam attenuation, $c(\lambda)$, coefficients of dissolved and total particulate substances are now routine in oceanographic research (Babin et al., 2008; Moore et al., 2008; see also Dickey et al., 2006). Spectral beam attenuation and absorption coefficients are inherent optical properties (IOPs)—their functional dependence is solely determined by the medium itself (in this case water and its constituents; Preisendorfer, 1976; Kirk, 2010). Spectral absorption in natural water is typically divided into four operational groups: $a_{\mathrm{TOT}} = a_{\mathrm{w}} + a_{\mathrm{CDOM}} + a_{\phi} + a_{\mathrm{NAP}}$ (m^{-1}), where the subscripts account for pure water (w), chromophoric-dissolved organic matter (CDOM), phytoplankton (ϕ), and nonalgal particulate matter (NAP); wavelength dependency is assumed but suppressed for brevity. Noting that in situ equipment is currently limited to measuring CDOM and total particles, laboratory and modeling techniques have been developed to partition total particle absorption into phytoplankton and NAP coefficients ($a_{\mathrm{p}} = a_{\phi} + a_{\mathrm{NAP}}$). The beam attenuation coefficient (summation of scattering and absorption) is partitioned in a similar manner, where only particles and water are assumed to contribute to light scattering ($c = c_{\mathrm{p}} + c_{\mathrm{CDOM}} + c_{\mathrm{w}}$, with $c_{\mathrm{CDOM}} \approx a_{\mathrm{CDOM}}$). Finally, the optical properties of pure water are well established (e.g., Morel, 1974; Pope & Fry, 1997) and are not considered a source of variability except temperature and salinity effects (e.g., Sullivan et al., 2006).

Many of the abovementioned IOPs have been shown to be correlated with biogeochemical parameters in marine waters. For example, the particle beam attenuation coefficient (c_{p}) in the open ocean is used as an index for particulate organic carbon (Gardner et al., 1993), and Boss et al. (2001b) found a relationship between the spectral shape of c_{p} and the particle size distribution (PSD). With respect to CDOM, compositional aspects (high vs. low molecular weight) can be inferred from the slope of its spectra (Carder et al., 1989; Blough & Del Vecchio, 2002), and in coastal waters CDOM covaries with the concentration of dissolved organic matter (Coble, 2007). Chlorophyll biomass can be estimated using the particulate absorption line-height at 676 nm (Davis et al., 1997). The relative estimate of PSD from c_{p} also provides insight on the dominant class of particles (i.e., size and composition by combining PSD with the backscattering ratio—see Twardowski et al., 2001;

Boss et al., 2004). Noteworthy of the NAP absorption coefficient is its featureless decaying spectra (e.g., Babin et al., 2003), which permits a_p to be partitioned numerically into phytoplankton and NAP (e.g., Roesler et al., 1989; Bricaud & Stramski, 1990; Hoepffner & Sathyendranath, 1993; Oubelkheir et al., 2007). The phytoplankton absorption coefficient has been used to estimate the relative size of the phytoplankton (Ciotti et al., 2002), and possible phylum identification through select pigment structures based on derivative analysis (Millie et al., 1997) or Gaussian decomposition techniques (Hoepffner & Sathyendranath, 1991; Ficek et al., 2004; Moisan et al., 2011).

The optical characteristics of temperate lake water have largely been limited to discrete laboratory measurements using bench-top spectrophotometry (e.g., Perkins et al., 2009), while the presentation of in situ IOPs are rare and often associated with unique lake systems, such as ultra-oligotrophic: Lake Taupo, New Zealand (Belzile et al., 2004) and Crater Lake, USA (Boss et al., 2007); or the Laurentian Great Lakes (O'Donnell et al., 2010). Here, we expand on these efforts with an extensive in situ optical dataset spanning 3 years between spring and fall (April–October) from four temperate lakes ranging from oligotrophic to eutrophic. Our focus is on temperature and hyperspectral (400–730 nm) measurements of total and filtered absorption and beam attenuation coefficients as a function of depth. A customized partition algorithm allowed us to estimate the in situ phytoplankton absorption coefficient and aided our ability to isolate and identify (qualitatively) dominant algal groups with distinct pigment biomarkers (e.g., phycobilins). Supplemented with backscattering and radiometric measurements, particulates were analyzed in the context of biogeochemical (e.g., size and composition) and ecological information (e.g., pigment variability) as a function of depth and time, both within and across the four lakes.

Methods

Sampling and site description

Between 2005 and 2007, four lakes in the central region of Upstate New York (Fig. 1) were profiled using an instrument package that included a 25 cm pathlength AC-s attenuation–absorption meter and a BB9 backscattering meter (WET Labs, Inc.), along with a CTD sensor (Sea-Bird Electronics). Onondaga Lake (ON), Otisco Lake (OT), Owasco Lake (OW), and Skaneateles Lake (SK) are dimictic, alkaline, hard water (calcareous) systems, varying from eutrophic to oligotrophic, respectively (both OT and OW are considered mesotrophic); lake characteristics are provided in Table 1. In 2005, the lakes were sampled approximately weekly starting in May (ON and OT) or monthly starting in June (OW and SK), all lasting through October. In 2006, weekly sampling occurred at ON from April through October and bimonthly at OT, OW, and SK from April through August. In 2007, sampling was reduced to ON (weekly) starting in May, and SK (biweekly) starting in April; both were sampled through October. Each lake were profiled at fixed locations near the center (widthwise; see Fig. 1), consisting of a single cast measuring the total (relative to water) spectral attenuation, $c(\lambda)$ and absorption, $a(\lambda)$ coefficients, followed by a second cast with a 0.2 μm (or prior to June 2006, a 0.45 μm) filter placed on the intake port of the absorption meter to effectively measure the CDOM absorption coefficient, $a_{CDOM}(\lambda)$. In addition, the BB9 meter measured the volume scattering function, $\beta(124°, \lambda)$, at nine discrete wavelengths (412, 440, 488, 510, 532, 595, 650, 676, and 715 nm). Between 2006 and 2007, underwater downwelling spectral irradiance and upwelling radiance was also measured using a hyperspectral radiometer system (Profiler II; Satlantic, Inc.). Finally, at each deployment discrete samples were collected at a depth of 2 m using a Kemmerer (or similar) water sampler and stored in 4-l polyurethane containers under cold dark conditions until laboratory measurements could be made (usually within 24 h).

AC-s and BB9 measurements

The AC-s has an approximate wavelength resolution of 4 nm from 400 to 730 nm (with a 15 nm bandwidth smoothing filter applied by the instrument's firmware), and is factory calibrated to air and pure water at a fixed temperature. For much of 2005 and 2006, predeployment utilized the *air*-calibration method as outlined by the manufacturer (AC-s Users Guide, Revision C) to correct for instrument drift. Regrettably, residual moisture within the optical tubes made it difficult to stabilize the measurement to within the instruments' repeatability (0.005 m^{-1}) resulting in

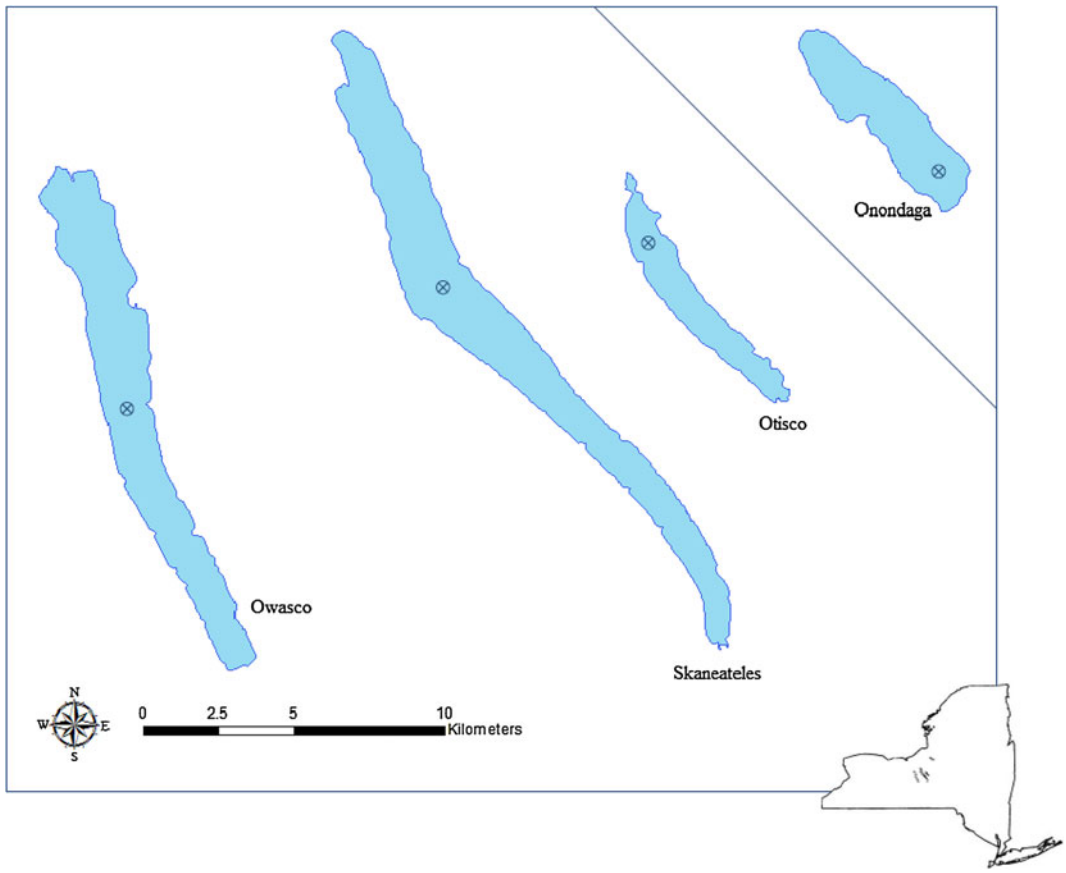

Fig. 1 Geographic location of the four lakes in New York State. *Hatch mark* shows general proximity of sampling station. See Table 1 for details

Table 1 Description[a] of lakes

Lake	Label	Location[b] (lat/long)	Volume (10^6 m^3)	Surface area (km^2)	Max depth (m)	Watershed (km^2)	Retention time (years)	Trophic status[a]	Secchi depth[d]	Comments
Onondaga	ON	43°04′43″ 76°11′50″	131	12.0	19.5	642	0.25	Eutro	1.8	Superfund site (Hg contam.)
Otisco	OT	42°52′07″ 76°17′40″	78	7.6	20.1	93.8	0.5	Meso	3.4	Drinking supply
Owasco	OW	42°50′30″ 76°30′45″	781	26.7	53.9	470	1.5[c]	Meso	3.8	Drinking supply
Skaneateles	SK	42°55′42″ 76°25′12″	1,563	35.9	90.0	154	7	Oligo	7.1	Drinking supply (no filtration)

[a] *Source* Upstate Freshwater Institute (www.ourlake.org)

[b] Location of monitoring buoy and AC-s measurements

[c] Flushing rate controlled by a dam

[d] Contrast measurement done facing the sun; average values reported in meters for 2006 only

variability between successive calibrations. This made the use of individual calibrations questionable. To circumvent this problem each set of air-calibrations per sensor between successive factory calibrations were combined in a linear model (by regressing the calibration values at each wavelength with time) to provide instrument drift as a function of Julian Day. Based on this approach each sensor appeared to drift in a similar manner in 2005 (~0.01 m^{-1} per month @ 410 nm), but in the following year the drift decreased roughly in half for the absorption sensor while staying the same for the attenuation sensor. A test of model accuracy by comparing predictions to factory re-calibration in August 2006 found on average the difference in correction for absorption was ± 0.005 m^{-1} and for attenuation ± 0.01 m^{-1}. (The relative offsets from the factory re-calibration in September 2005, exceeded model predictions—greater than a factor of two, suggesting additional instrument drift may have occurred in transit). In addition, on several occasions in 2006 (between mid-June and August), the instrument was calibrated using de-ionized (18 MΩ nominal) water as described by Twardowski et al. (1999). Both air and water methods agreed favorability ($\leq \pm 0.005$ m^{-1}). In 2007, water calibration became the default calibration method and was performed directly before or after each deployment.

After a warm-up phase of 5 min, each cast started at a depth of 1 m, descended to within a few meters of the bottom (ON/OT) or to nearly 35 m (OW/SK). To maximize the signal-to-noise in the AC-s spectra, the instrument package was lowered manually at an approximate rate of 1–2 m/min (to obtain >50 scans per 1 m bin interval). A second cast, pumping water only through the a-tube with a (Gelman suporcap 100) pre-filter on its intake, followed within 20 min. Although it was standard procedure to purge the filter for several minutes, many profiles displayed discontinuities in the absorption spectra (near 565 nm; the overlap region between the two linear optical filters in the AC-s) and thought to be entrapped bubbles in the filter generating excessive light scattering; such spectra were later discarded.

AC-s and BB9 measurements were merged with pressure and temperature data using the manufacturer's extraction software (WAP). The volume scattering function was converted to the particle backscattering coefficient (b_{bp}) according to recommendations provided by the manufacturer (WET Labs, Inc., 2008). The entire dataset was binned into 1 m depth intervals using a ± 0.5 m averaging window subjected to a trimmed (75 percentile) mean. Post-processing utilized two distinct methods. The calibration-dependent procedure applies to the particle attenuation coefficient because it does not utilize the same sensor for total and filtered measurements ($c_p = c - a_{CDOM}$). Here, the above mentioned calibration offsets are applied to each channel as well as corrections for temperature effects for absorption by pure water (using Sullivan et al., 2006).

The calibration-independent method (Boss & Zaneveld, 2003; Boss et al., 2007) assumes calibration offsets are effectively nulled if total and filtered measurements are obtained from the same optical sensor, which for our data set was only applicable to the particle absorption coefficient ($a_p = a - a_{CDOM}$). Since the time difference between casts could produce residual temperature differences, we followed the method described by Slade et al. (2010) for simultaneous scattering and temperature correction. For the scattering correction we applied the 'proportional' method from Zaneveld et al. (1994), where a_p is assumed to be zero at 720 nm. Note that, the scattering correction step used here does require the particle scattering coefficient (b_p) computed using the calibration-dependent total attenuation and absorption coefficients ($b_p = c_p - a_p \equiv c - a$). Finally, discarded CDOM spectra due to bubble error were replaced by the nearest acceptable CDOM spectra in the profile for the purpose of calculating a_p (and c_p).

Radiometric measurements

In 2006 and 2007, the OCR-3000 series radiometric sensors (Satlantic Inc.) were used to measure subsurface downwelling irradiance (E_d) and above surface irradiance (E_s). Deployment adhered to protocols described in Mueller (2003). The E_d sensor was attached to a free-falling profiling frame, while the reference (E_s) sensor was manually fixed to a vertical mount onboard in a location that minimized shadowing. Data was recorded, along with corresponding pressure and temperature information using Satlantic's data control and logging software. The unit was deployed on the sunny-side of the boat at an approximate rate of 0.2 m s^{-1} as recommended by the manufacturer for inland waters. Calibration of the sensors occurred in 2005 and 2007 (but drift of similar

instruments has been found to be smaller than 2% year^{-1}; see Voss et al., 2010); absolute accuracy, however, was not critical to our primary use of the data (see below).

Post-processing of radiometric data was done with the manufacturer software (ProSoft). User supplied inputs for the irradiance reflectance albedo (combined sun and sky; unitless) and the refractive index for freshwater were set to 0.04 and 1.334, respectively. Relative and absolute PAR (photosynthetic active radiation; units: µmols m^{-2} s^{-1}) were then calculated at 0.5 m intervals to determine depths corresponding to 1% PAR (denoted Z_{MIN}). For reference, in 2006 and 2007, 1% PAR levels varied between 2.6 to 21.9 µmols m^{-2} s^{-1}.

When radiometric measurements were unavailable, the algorithm of Lee et al. (2007) using measured IOPs (a(490) and b_b(490)) was used to estimate the depth associated with 1% PAR. The required solar (zenith) angles were computed according to Iqbal (1983). When comparing Lee's algorithm estimates with data from 2006 and 2007, discrepancies in Z_{MIN} were noted and found on average to be in excess of 1–2 m in the least productive lake (SK).

Discrete measurements

Water collected from each lake at 2 m below the surface during 2005 and 2006 was analyzed in a laboratory for absorption of total particle (a_p) and NAP (a_{NAP}) in the spectral range of 400–750 nm using a specially designed spectrophotometer (PerkinElmer 18 dual-beam spectrophotometer configured with a 150 mm integrating sphere, Labsphere RSA-PE-18). Sample preparation involved the quantitative filter technique (QFT) as outlined in the NASA protocols for discrete particle absorption (Mitchell et al., 2003), and the measurement process is covered in detail elsewhere (Kalenak, 2011). Noteworthy is the procedure utilized the bleaching method (5 min soak in a 5% sodium hypochlorite solution) to remove pigments and the path-length scattering correction was done according to Cleveland & Weidemann (1993). The phytoplankton absorption coefficient was obtained by difference ($a_\phi = a_p - a_{NAP}$). An estimate of chlorophyll a ([Chl a]) was made using the absorption line height at 676 nm as described in Boss et al. (2007). Spectra were normalized by the area below curves (e.g., Roesler et al., 1989) to minimize concentration effects and obtain information on their shape. We binned the normalized spectra into three levels for each lake based on [Chl a], corresponding to a 'low', 'medium, and 'high' range using the 33 and 67 percentiles of the combined 2 year dataset. (The 33/67 percentiles equated to 11.1/15.0, 3.0/4.7, 1.1/2.6, and 0.64/0.94 mg m^{-3} for ON, OT, OW, and SK, respectively.) The normalized laboratory spectra were then binned according to these partition levels and averaged to create a three-tier set of (four) lake-specific basis vectors ($\bar{a}_\phi$). This last step was intended to mitigate potential error associated with the package effect (Kirk, 2010) which has the effect of flattening a_ϕ in the blue as a function of increasing [Chl a] (see 'Results' section).

Phytoplankton partition model

To obtain the best estimate of absorption by algal and non-algal particles, we partitioned in situ a_p coefficient into the fraction representing phytoplankton and non-algal particles based on a two-component end-member algorithm (e.g., Hoepffner & Sathyendranath, 1993) using the expression: $a_p^{AC\text{-}s}(\lambda) = C_0\bar{a}_\phi(\lambda) + C_1\exp(-C_2(\lambda - \lambda_r)) + C_3$. The middle term represents a_{NAP} and basis vector ($\bar{a}_\phi$) is obtained from the above described laboratory spectra, while the constant term was introduced to constrain particle absorption to zero in the NIR (e.g., Estapa et al., 2012). The goal of this algorithm was to estimate NAP absorption, by optimizing the expression for parameters C_0–C_3 using the lake-specific $\bar{a}_\phi$ tiered to the corresponding chlorophyll level in a_p. The function fitting was done using a least-square minimization (fminsearch in Matlab®) in the wavelength range of 420–720 nm. The absorption coefficient for phytoplankton, $a_\phi(\lambda)$, was then obtain by subtracting this part of the end-member model from the AC-s measurement: $a_p^{AC\text{-}s}(\lambda) - (C_1\exp(-C_2(\lambda - \lambda_r)) + C_3)$. In cases where C_1 was negative or if C_2 fell below 0.005 nm^{-1}, the computation was repeated using a fixed slope value for C_2—0.011 nm^{-1} (based on extensive measurements by Babin et al., 2003), which occurred 62 times (4%) in 1,722 spectra that comprised the final data set. To help gauge the sensitivity in the initial estimate of the NAP absorption coefficient, two additional NAP spectra were also computed simultaneously after applying ±1 sigma (from laboratory spectra) to the basis vector $\bar{a}_\phi$. (We found that the model showed significant sensitivity

when estimating NAP when the measured spectra was predominately (>75%) phytoplankton as inferred by the line-height at 440 nm, provided the 676 nm absorption line-height for particle absorption was $>0.01\ m^{-1}$). From a total of 1,940 initial spectra, 218 computed a_ϕ spectra (~11%) were discarded using the criteria: (1) if NAP was negative or (2) if a_ϕ was negative or its amplitude was degraded by noise. The latter issue often occurred if the 676 nm (chlorophyll) peak dropped below $0.005\ m^{-1}$, which typically happened at depths below 1% PAR (e.g., 71% of the rejected spectra came from the bottom 5 m). In the final step, the accepted spectra were subject to a single pass peak-preserving smoothing filter to remove residual noise (Savitzky & Golay, 1964; settings: $K = 5$, $F = 15$).

We recognize that the above process is not perfect. Beyond uncertainties associated with QFT (e.g., scattering correction, procedural, and handling issues, etc.; see Roesler, 1998), the lab spectra used to compute $\bar{a}_\phi$ all came from near the surface. However, since the purpose of the decomposition method employed here is to reveal the *shape* of the phytoplankton absorption coefficient from total particle absorption (by removing the best estimate of NAP from the particulate measurement), we feel the approach is justified (see discussion).

Supplemental analytical methods

The spectral shape of c_p has been shown to be related to the PSD. For example, Boss et al. (2001b) found that if the size distribution of particles can be approximated by a power-law (e.g., $f(D) \sim D^{-\xi}$), the exponent of a power-law fit to $c_p(\lambda)$ can be used to estimate the size parameter ξ. We used their relation to computed ξ which was then used as a measure of the relative changes in particle size (e.g., Boss et al., 2001a); where, for example, if ξ trended higher (lower) this shift represents a decrease (increase) in particle size. In addition, $c_p(660)$ was used as an index of *total* suspended particle mass (SPM; see review by Hill et al., 2011), which is affected by both biogenic and inorganic substances.

The particle backscattering ratio ($b_{bp}^R = b_{bp}/b_p$) was used to assess whether particle assemblages were comprised mainly of algal cells ($b_{bp}^R < 1\,\%$) or minerogenic substances ($b_{bp}^R > 2\,\%$; Twardowski et al., 2001; see also Whitmire et al., 2010). To avoid effects related to absorption (Boss et al., 2004), only the 650 nm channel on the BB9 was used to compute b_{bp}^R.

We estimated *total column* chlorophyll concentration by summing the individual (binned) [Chl *a*] values over the entire profile (denoted [ΣChl *a*]; mg Chl *a* m^{-2}).

The estimated phytoplankton absorption spectra often exhibited spectral peaks that varied with depth. To determine their amplitudes, we applied a technique similar to estimating [Chl *a*] by computing the line-height of the peak relative to a baseline through two adjacent points in the absorption coefficient. The most prominent peaks were found at 545, 560 (and specific to SK, 575), and 625 nm; wavelengths assigned to the corresponding baseline were located at ±15, −20/+30, ±15 nm (respectively), except for the 575 peak where a narrower bandwidth of ±10 nm was used. The acceptance threshold for detection was set to the standard error of the mean in a_p at the abovementioned wavelengths (which was relatively consistent for each lake: 0.0025, 0.0020, 0.0008, and $0.0010\ m^{-1}$ for ON, OT, OW, and SK, respectively). Lastly, because the location of the peak amplitude was observed to vary slightly across spectra, the peak value was chosen as the maximum value after shifting the computation by ±2 nm.

Uncertainty in the values reported

The AC-s has a specified uncertainty of $\pm 0.01\ m^{-1}$, but does occasionally exhibit a much higher variability in the blue wavelength region ($\lambda < 440$ nm) because of lower lamp output. Although the number of scans per binned depth was large, the average standard error of the mean (SE) for $a_p(410)$ was on the order of $0.005\ m^{-1}$ with a maximum (95 percentile) of $0.02\ m^{-1}$, but dropped to $0.002\ m^{-1}$ at 660 nm. For $c_p(410)$, SE was 0.01 with a maximum of 0.05 and a similar decrease at 660 nm. We therefore assume the level of uncertainty in a_p and c_p is reasonably close to the instruments' specification ($\pm 0.01\ m^{-1}$), but recognize that variations in scattering correction methods applied to absorption measurements can result in uncertainties on the order of 30% in the blue. As a conservative measure we assigned a combined uncertainty of ca. $\pm 0.015\ m^{-1}$ to the particle absorption coefficient and ca. $\pm 0.02\ m^{-1}$ to the particle beam attenuation coefficient.

Uncertainties associated with an erroneous estimate of NAP could bias the computed phytoplankton absorption spectrum, particularly in the blue. Estimating this uncertainty was done by comparing the decomposition method with the NAP spectra obtained from laboratory measurements, with the caveat that the level of uncertainty in the QFT measurements is unknown and likely not insignificant (e.g., Roesler, 1998; see also Kalenak, 2011). Relative to the average, the RMSE between the NAP amplitude at 410 nm for discrete and modeled 2 m spectra was 19, 14, 42, and 42% for ON, OT, OW, and SK, respectively. For the NAP slope parameter, the relative RMSE was 10, 11, 26, and 13% (respectively). Overall, the amplitudes of the modeled estimates were systemically higher, while the slope values were generally biased low. For the purpose of the current study, because we focused on the spectral features in the phytoplankton absorption coefficient, these uncertainties are not significant since the absorption spectra of NAP are smoothly varying (e.g., Nelson & Robertson, 1993). In addition, the magnitude of the above errors is consistent with other partitioning algorithms (see Zhang et al., 2009).

Uncertainties in our estimate of chlorophyll are on the order of ±50% or possibly higher given the variability in specific absorption of phytoplankton at 676 nm (here assumed to be 0.014 m^2 (mg Chl a)$^{-1}$; Bricaud et al., 1995; see also Johnsen & Sakshaug, 2007). The uncertainty in pigment amplitude line-heights are thought to be less than 0.001 m^{-1} based on precision of the AC-s (0.005 m^{-1}) and the above mentioned SE's.

Results

Annual cycle in hydrography

The three lakes we have data for in early spring (e.g., April) were all well-mixed (see Fig. 2a–d). Stratification began in May for ON, OT, and OW, but was not apparent until June in SK. Maximal thermal separation between the epilimnion and hypolimnion generally occurred in the months of July and August, but extended into September for SK. For all systems, falling temperatures in October weakened the thermocline, although the extent varied over the sampling period.

By inspection (all cases), the approximate depth of the epilimnion in ON ranged from 5 m during maximum stratification to over 8 m in September. For the same period in OT (2005), the range was 7 m to greater than 12 m. OW generally had epilimnetic depths exceeding OT by 2–3 m and displayed similar seasonal changes in thermal layering. In contrast, the epilimnion in SK continuously deepened until October, at which it was often greater than 20 m. A consistent hypolimnetic layer in ON had an upper boundary near 10–12 m, separated by a large metalimnion—usually greater than 4 m. Unlike ON, this boundary was more varied in OT—starting at 8–10 m in July/August but dropped to over 13 m in September, often accompanied by a sharp metalimnion (~1 m). For OW, the hypolimnion was typically below 15–20 m and usually associated with a relatively weak temperature gradient spanning 5–6 m. The strongest metalimnions (<1 m) were observed in SK, where the hypolimnic region typically started at depths below 25 m.

Chlorophyll distribution

Over the sampling period (2005–2007 for ON and SK, 2005–2006 for OT and OW), Chl a concentration ([Chl a]) varied from 0.1 to 34 mg m^{-3} in ON, 0.3–16 mg m^{-3} in OT, 0.2–13 mg m^{-3} in OW, and 0.1–3 mg m^{-3} in SK (Fig. 2; Table 2). When data was available, vertical gradients were observed to be minimal prior to stratification (between April and May), while variations between successive samples was small except for ON which exhibited a large decrease from ca. 25–6 mg m^{-3} in April, 2006 (Fig. 2a). Localized chlorophyll maxima became apparent once the lakes began stratifying, and most notably modulated into algal blooms in July 2005 for ON and OT, where [Chl a] reached 30 and 15 mg m^{-3}, respectively; both events weakened but persisted into August. A moderate increase in [Chl a] was also observed for the same time period in OW. However in early June 2006, a chlorophyll maximum located at 10 m evolved 2 weeks later into a modest bloom centered at 2 m and measured 13 mg m^{-3}. The bloom appeared to collapse in the following month, but [Chl a] increased back to 9 mg m^{-3} in August. In July of the same year, pronounced changes (relative to an oligotrophic lake) were observed in SK, both within and below the epilimnion, ranging from less than

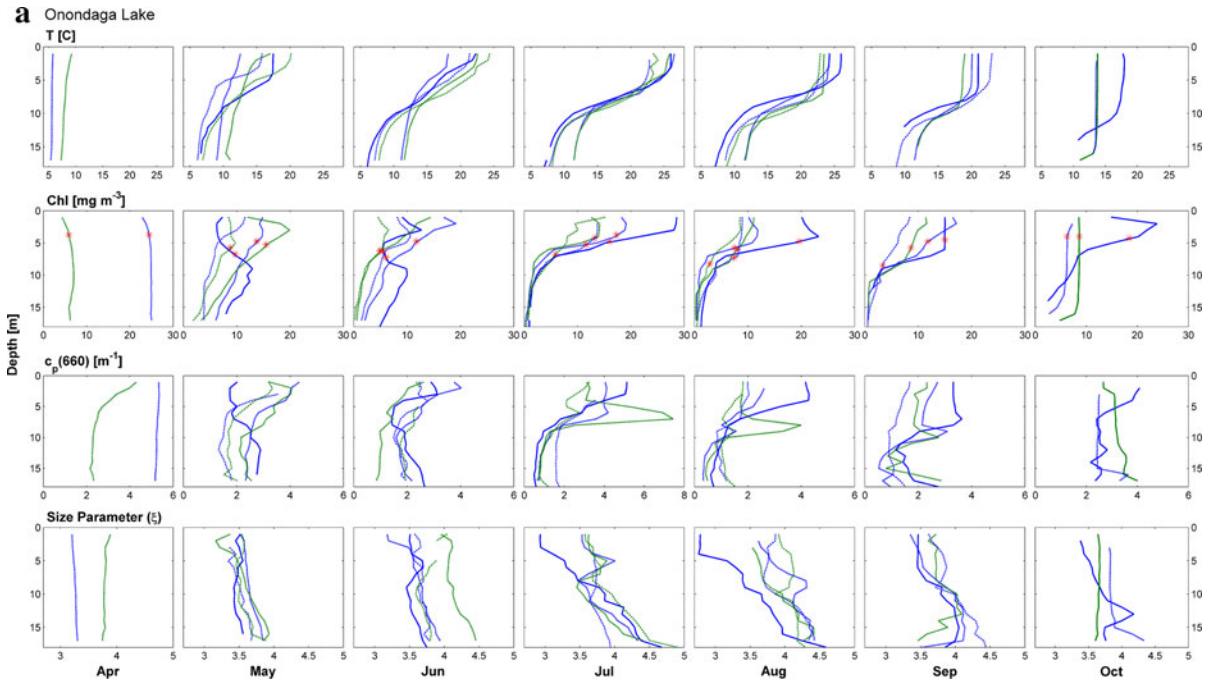

Fig. 2 Monthly waterfall plots for April–October. Onondaga Lake (2005–2007): **a** temperature (C°); **b** Chl *a* concentration (mg m^{-3}) based on the phytoplankton 676 nm absorption line-height (see text), along with measured or estimated Z_{MIN} depth (*); **c** particulate beam attenuation coefficient at 660 nm (m^{-1}); **d** particle-size parameter (ξ). To match bimonthly sampling frequency of other lakes, profiles were averaged in a sequential manner if the number exceeded more than two per month; and in months when there was five profiles, the last three were averaged. Line key: *solid curve* 2005, *dashed curve* 2006; *dash-dot curve* 2007. *Color code*: *blue* represents the first sample in each month, *green* represents the second. Otisco Lake (2005–2006): as in **a** (ON) except no averaging. Alternative *top x axis* (with modified *color*) is provided in special cases. *Note* some profiles are incomplete. Owasco Lake (2005–2006) as in **b** (OT). *Note* no data were available for April. Skaneateles Lake (2005–2007) as in **b** (OT). *Note* any Z_{MIN} value exceeding the range of the AC-s profile is not shown

1–3 mg m^{-3}. Most notable for SK was the deep chlorophyll maximum (DCM) in August of 2005 measuring 2 mg m^{-3} and centered at 24 m just above the depth corresponding to 1% PAR (model estimate for Z_{MIN} was 32.5 m). Colder temperatures and deepening of the epilimnion (breakdown of stratification) in late October produced lower and more uniform [Chl *a*] levels in all four lakes, except for ON and OT in 2005, where in the first half of the month algal biomass was both elevated and exhibited large vertical structure in the upper layer.

In all lakes except SK, once stratification became pronounced depths associated with 1% PAR (Z_{MIN}) were generally found along the base of the metalimnion (Fig. 2); for SK, Z_{MIN} was often located in the upper region of the hypolimnion (>25 m). For ON, Z_{MIN} varied between 4 and 6 m, but on several occasions exceeded 8 m (Table 2). In OT, Z_{MIN} was at or below 10 m except for the bloom event in 2005 where it decreased to <6.5 m. The typical value of Z_{MIN} in OW was similar to upper range in OT (13–15 m) except in August, 2006, where it dropped to 3 m; noteworthy because of the comparatively modest level of [Chl *a*] present at that time. Across all of the four lakes in almost every profile, the relative level of Chl *a* remained elevated below Z_{MIN}, often by several meters.

Integrated chlorophyll

Segmented by month, the entire span of the a_p profiles for each lake were used to determine the total column integrated chlorophyll concentration per unit area ([ΣChl *a*]) and that associated with depths below Z_{MIN} (Fig. 3). Relative to their monthly average, all four lakes exhibited a factor of two or more in variability. The spring and fall standing stock of biomass in ON was significantly larger than the other lakes, ranging from 150 to 260 (mg Chl *a*) m^{-2}, of which the majority

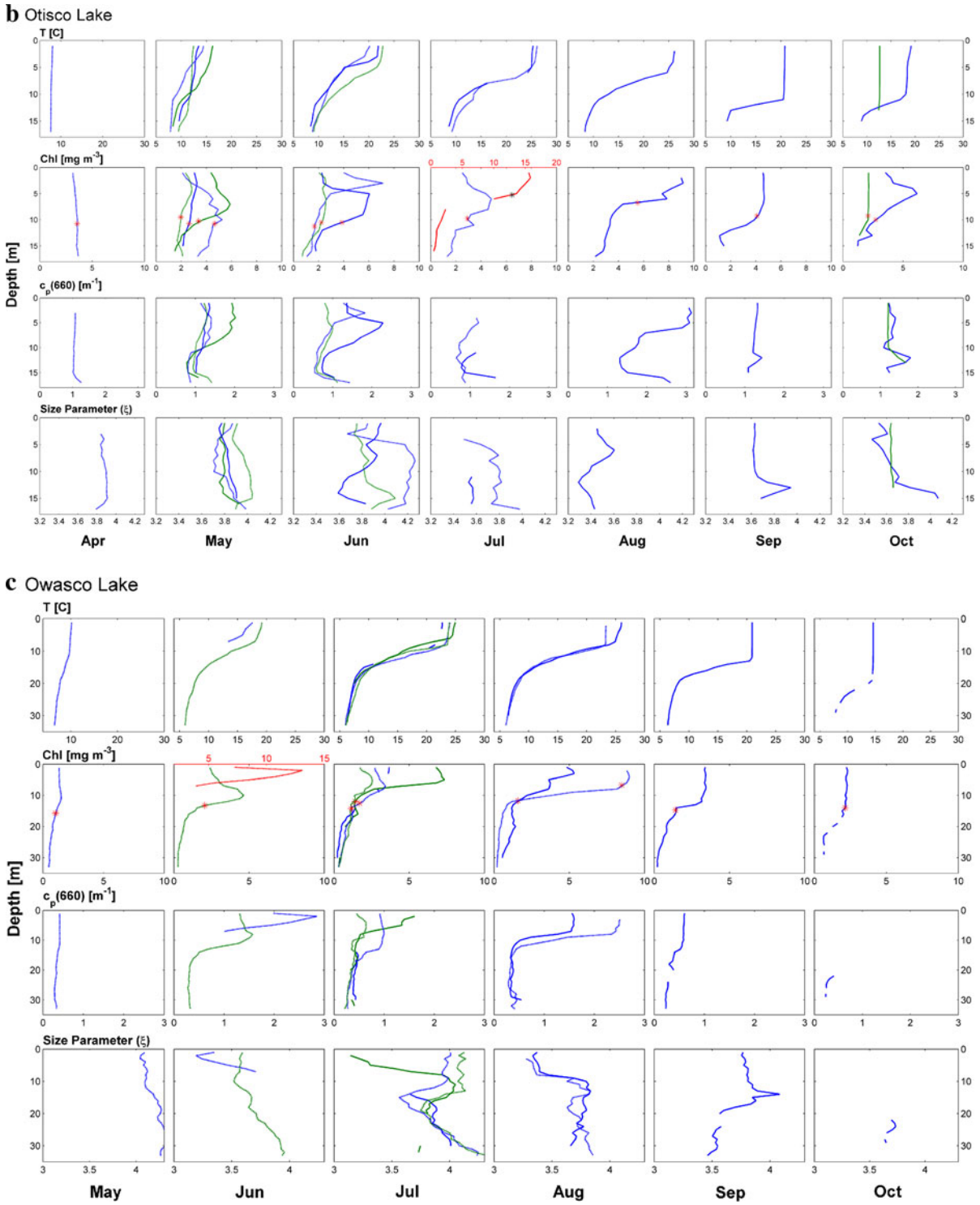

Fig. 2 continued

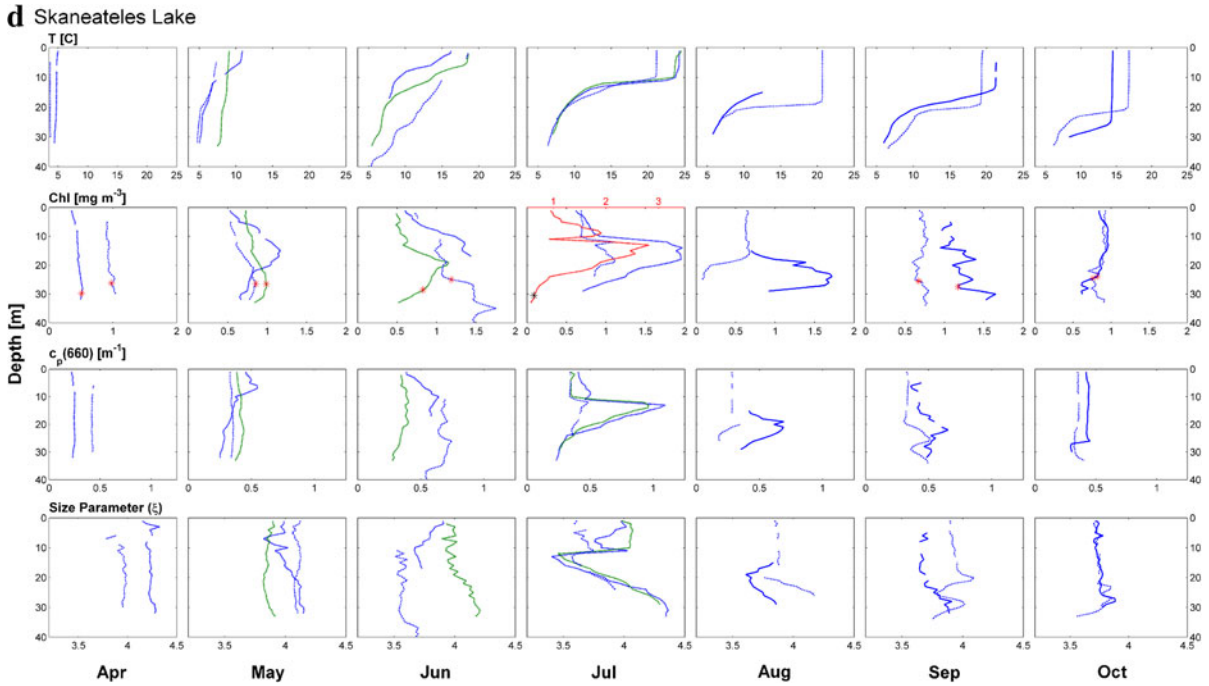

Fig. 2 continued

was found below Z_{MIN}. The least productive (and consistent) system was SK with an overall average of 25 (mg Chl *a*) m^{-2}, and here much of the observed biomass was above Z_{MIN}. For both OT and OW, the typical value for [ΣChl *a*] was around 55 (mg Chl *a*) m^{-2}, where less than half was present below Z_{MIN}, and this was especially true during the peak summer months. Noteworthy of this time period (June through August) was the small variation in the average value of [ΣChl *a*] for ON, and only modest (average) changes in both mesotrophic systems; in SK, the observed minimum of [ΣChl *a*] occurred in month of August.

Particle size and concentration

The spectral shape of the normalized beam attenuation coefficient was consistent with the trophic status of the four lakes (Fig. 4a). The slope of the c_p spectra was smallest in the most productive lake (ON) indicating a larger bulk particle size, and steepest in the least productive lake (SK) implying a dominant class of smaller particles.

Once ON stratified, the particle-size parameter (ξ) generally increased with increasing depth (Fig. 2a) suggesting particles at depth were smaller. Variability was highest at the metalimnion between the months of June through August, though a sizeable modulation was observed in the upper water column in May (2006) coincident with an increase in chlorophyll concentration. Large changes were also observed in several profiles near the bottom of the lake during September and October. The size parameter changed markedly in association with the bloom and its collapse in the summer of 2005 (July through September), while the October increase in [Chl *a*] appeared to have only a minor effect. Overall, the inverse correlation between ξ and [Chl *a*] was weak but significant ($r^2 = 0.51$; $P < 0.0001$).

In the months of April through June $c_p(660)$ tracked well with changes in [Chl *a*], and clearly registered the algal bloom that occurred in 2005. A sizeable increase in $c_p(660)$ at the metalimnion coincided with a large influx of terrestrial particles from a severe weather event in early July 2006 and persisted into September; no evidence of this event was found in the corresponding [Chl *a*] profile. In September and October, several of the profiles ξ were observed to decrease approaching the bottom (larger particles) while $c_p(660)$ increased.

Table 2 Monthly range of select parameters

Lake	Parameter	April	May	June	July	August	September	October
Onondaga	[Chl *a*]	25.0–4.3 (15.6)	23.5–1.9 (8.6)	20.3–0.1 (4.3)	28.6–0.1 (2.6)	23.3–0.3 (3.2)	21.1–0.5 (7.6)	33.5–2.5 (8.0)
	ξ	3.9–3.2 (3.5)	4.1–2.8 (3.6)	4.6–3.1 (3.7)	4.9–2.9 (3.8)	4.6–2.8 (3.9)	4.4–3.3 (3.8)	4.5–3.3 (3.7)
	Z_{MIN}	3.9 (NA)	6.9–4.7 (6.0)	7.6–4.6 (6.3)	8.6–3.9 (4.9)	8.5–4.6 (6.3)	8.7–4.6 (6.1)	4.6–3.8 (4.1)
	$c_p(660)$	5.3–2.1 (3.7)	5.1–1.3 (2.3)	4.5–0.7 (1.8)	7.4–0.5 (1.4)	4.2–0.3 (1.2)	4.7–0.5 (1.9)	4.8–1.9 (2.8)
Otisco	[Chl *a*]	3.6–3.1 (3.5)	5.9–1.5 (3.4)	7.1–0.7 (2.4)	15.8–0.5 (2.4)	9.1–2.1 (3.4)	4.7–1.1 (4.3)	6.2–0.3 (2.9)
	ξ	3.9–3.8 (3.9)	4.0–3.7 (3.8)	4.3–3.6 (3.9)	4.0–3.5 (3.7)	3.6–3.3 (3.4)	3.9–3.6 (3.6)	4.1–3.5 (3.7)
	Z_{MIN}	10.9 (NA)	10.8–9.7 (10.4)	11.5–10.5 (10.8)	9.8–5.3 (7.5)	6.8 (NA)	9.5 (NA)	10.4–9.3 (10.0)
	$c_p(660)$	1.3–1.0 (1.1)	2.0–0.8 (1.3)	2.3–0.5 (1.0)	1.6–0.6 (0.9)	3.1–1.3 (1.9)	1.4–1.1 (1.3)	1.8–0.9 (1.2)
Owasco	[Chl *a*]	NA	1.5–0.5 (1.0)	13.1–0.3 (4.7)	7.3–0.2 (1.1)	9.0–0.2 (0.9)	3.4–0.2 (1.3)	2.3–0.6 (2.2)
	ξ	NA	4.3–4.0 (4.2)	4.0–3.2 (3.5)	4.3–3.1 (3.9)	3.9–3.3 (3.7)	4.1–3.5 (3.8)	3.7–3.5 (3.7)
	Z_{MIN}	NA	16.0 (NA)	13.3–8.7 (11.0)	14.5–11.6 (12.8)	11.9–7.0 (9.5)	14.9 (NA)	14.1 (NA)
	$c_p(660)$	NA	0.4–0.3 (0.3)	2.8–0.3 (1.2)	1.6–0.2 (0.4)	2.5–0.3 (0.4)	0.6–0.2 (0.4)	4.0–0.2 (0.3)
Skaneateles	[Chl *a*]	1.0–0.4 (0.7)	1.2–0.5 (0.8)	1.8–0.5 (1.0)	2.8–0.6 (1.1)	1.7–0.08 (1.0)	1.7–0.6 (1.0)	1.0–0.6 (0.9)
	ξ	4.3–3.8 (4.1)	4.2–3.8 (4.0)	4.2–3.5 (3.8)	4.4–3.4 (3.9)	4.2–3.6 (3.8)	4.1–3.6 (3.8)	3.9–3.6 (3.7)
	Z_{MIN}	29.9–26.3 (28.1)	39.1–26.5 (29.7)	28.7–25.0 (25.1)	35.5–27.2 (30.1)	32.6–28.3 (30.4)	27.7–25.6 (26.7)	24.7–23.9 (24.3)
	$c_p(660)$	0.4–0.2 (0.3)	0.5–0.3 (0.4)	0.7–0.3 (0.5)	1.1–0.2 (0.4)	0.7–0.2 (0.4)	0.7–0.3 (0.4)	0.5–0.3 (0.4)

Values represent the sampling period from 2005 to 2007; median shown in parenthesis unless insufficient data. [Chl *a*] has units of (mg m^{-3}), Z_{MIN} (m), and $c_p(660)$ (m^{-1})

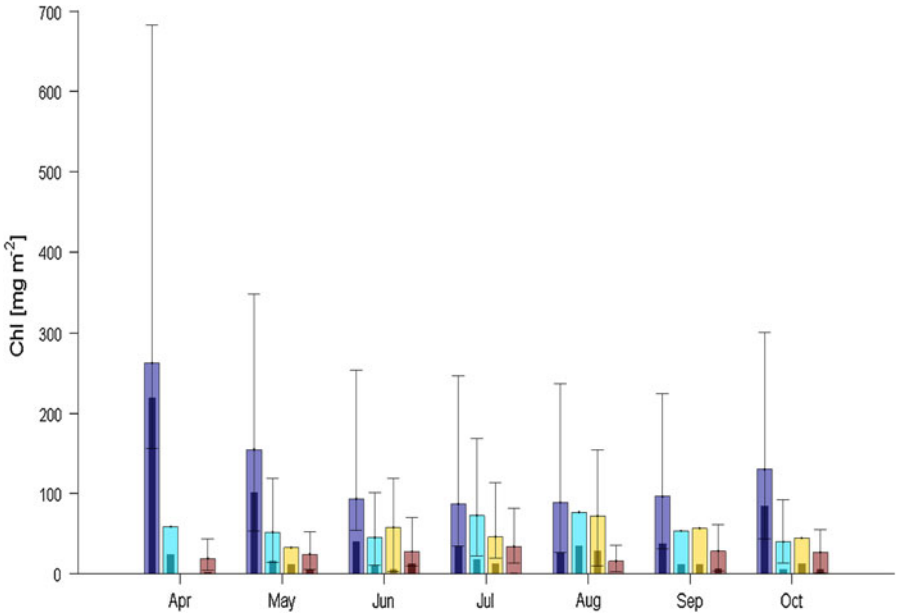

Fig. 3 Total column integrated Chl *a* concentration (per unit area based on the average for each month; mg Chl *a* m^{-2}). *Opaque inset* is the same except for depths below Z_{MIN}. *Error bars* represent max and min range (applicable to months with multiple profiles). Group order, *left* to *right* ON, OT, OW, and SK

Before stratification, OT exhibited vertical uniformity in particle size, although increased variability was evident in May (Fig. 2b, c). Modulation of ξ was strong in June, most notably in the upper layers coincident with large changes in the concentration of chlorophyll particles. Much of the variability in size parameter often occurred at/near the metalimnion (e.g., August and September), while an occasional downward trend in ξ was tightly correlated with an increase in chlorophyll (e.g., June, 2006 and October). Also, ξ exhibited large variation in June near the bottom boundary layer; the shift (approaching the bottom) was towards smaller particles in 2005 and larger particles in 2006, and a similar pattern repeated itself in October and September (2005, respectively).

In late May (2005) $c_p(660)$ was uniform in the upper 8 m compared to [Chl *a*], while in June $c_p(660)$ exhibited a localized maxima at 5 m with Chl *a* remaining nearly constant in the region from 5 to 10 m. As with ON, near the bottom of several profiles $c_p(660)$ was observed to increase relative to an increasing (e.g., June or August, 2005) or decreasing (e.g., June, 2006) particle-size parameter; changes in particle size were also made apparent by ξ near the base of the metalimnion in both September and October, 2005.

Throughout the entire sampling period, variation in both particulate and chlorophyll concentrations were consistent in OW (Fig. 2b, c). In 2006, the lake was dominated by a relatively uniform and somewhat smaller class of particles ($\xi > 4$), as compared to ON and OT. Instances of increased Chl *a* in June, July, and all of August varied inversely with the ξ (overall, $r^2 = 0.62$; $P < 0.0001$). Changes in ξ suggesting smaller size particles were also apparent along the metalimnion in September, opposite of that for the two profiles taken in July (both years). The size parameter was stratified in the more productive months between June and August and usually decreased with depth. End of the season profiles were more uniform and with lower values (consistent with larger particle sizes and similar to spring).

In SK, the size parameter displaying a general decrease with increasing [Chl *a*] was well coupled to changes in chlorophyll (Fig. 2d). For example, in April and May (all years), chlorophyll increased towards 1.0 mg m^{-3} with a corresponding decrease in ξ. The DCM in August was also evident in the ξ profile, but a 5 m offset between the two profiles indicated that the maximum shift in the particle size was better matched to the metalimnion and not [Chl *a*].

The decoupling of [Chl *a*] relative to particle mass was also evident in the $c_p(660)$ profiles for the DCM, as seen in May and June of 2006; particle maxima registered either above (similar to ξ) or was absent relative to the maxima the corresponding Chl *a* profiles. In addition, the upper layer modulations in [Chl *a*] for the modest bloom event in July (2006; 2.8 mg m^{-3}) were not evident in $c_p(660)$.

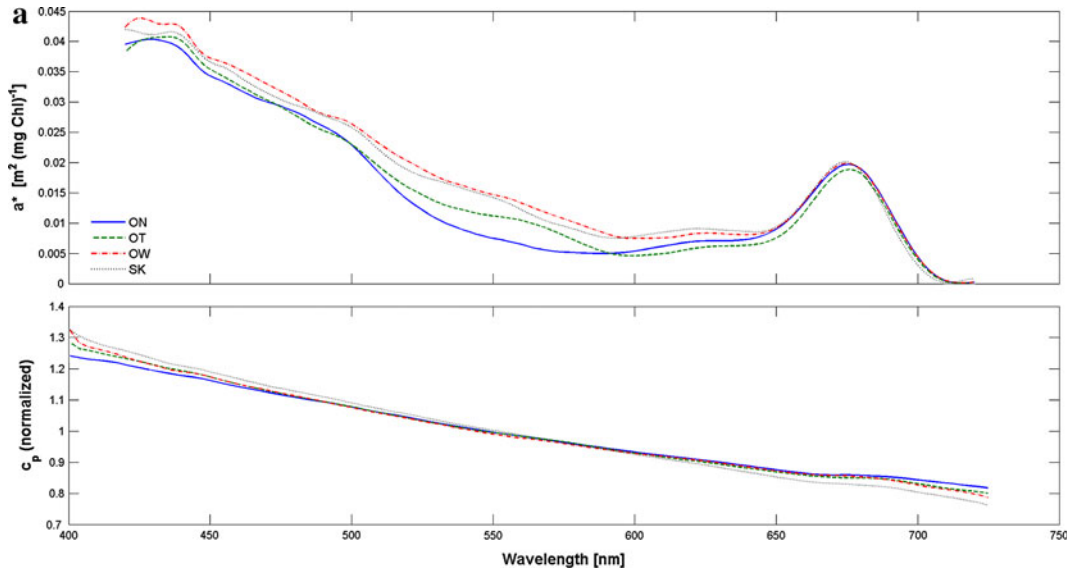

Fig. 4 **a** Average chlorophyll-specific phytoplankton absorption coefficient (m^2 (mg Chl *a*) $^{-1}$; $\lambda = 420$–720 nm; *top*) and average normalized (area) particulate beam attenuation coefficient (no units; $\lambda = 400$–730 nm; *bottom*). The entire data set for each lake was used to compute the average. *Note* a Savitzky–Golay filter ($K = 8$, $F = 15$) was applied to absorption spectra. **b** Normalized (676 nm) phytoplankton absorption coefficient (*left panel*). Select profiles from ON (June 18, 2007; $Z_{MIN} = 7.4$ m), OT (June 6, 2005; $Z_{MIN} = 10.5$ m), and SK (July 19, 2007; $Z_{MIN} = 28.2$ m; spectra represents the original set reduced by stepping 3 m and averaging the range from one above/below each step) to illustrate chromatic changes in a_ϕ (λ, *z*). *Right side* is a qualitative (waterfall) comparison of the amplitude line-height of select absorption peaks as a function of depth with Chl *a* concentration (*black*, *heavy solid*). *Note* to enhance visualization of the peak amplitudes relative to Chl *a*, a scaling factor (×4) was applied to ON (*top*) and SK (*bottom*). **c** Analysis of select pigment peaks in phytoplankton absorption spectra (*right panel*). Histogram (*top*) displays pigment occurrence (%) in a_ϕ spectra per lake segmented by Z_{MIN}. Time series (*bottom*) shows the monthly average amplitude line-height of the three pigment peaks (545, 560, and 620 nm) in each lake. Represented is the entire data set (2005–2007)

Spectral features in the phytoplankton absorption coefficient

To highlight spectral features of the bulk phytoplankton (e.g., Bricaud et al., 1995), we normalized the absorption spectra to the corresponding [Chl *a*] (Fig. 4a). The lake-averaged chlorophyll-specific absorption coefficient (denoted by a_ϕ*) exhibited features characteristic of Chl *a*, most notably broadband absorption peaks in the blue (440 nm) and red (676 nm). Of varying degree each of the lakes also exhibited shoulders centered near 450 and 500 nm, and a broad subtle peak centered at 620 nm. Both OW and SK appeared to contained more light-harvesting accessory pigments in the green, while ON displayed the largest amount of the 'package effect' (Duysens, 1956; see also Kirk, 2010) as evident by a smaller blue-to-red ratio (440:676 nm).

As soon as the water column stratified, the shape of phytoplankton absorption spectra was observed to vary with depth; three distinct examples (Fig. 4b) were chosen to showcase these chromatic changes in a_ϕ. In mid-June (2006), the ON spectra exhibited flattening in the blue (an increase in packaging) which appeared to reach a maximum around 7 m. A subtle shoulder was present in many of the spectra near 490 nm. The most prominent spectral feature occurred near 560 nm, becoming significant below 4 m and by 6 m its magnitude was roughly one-quarter of the corresponding Chl *a* peak at 676 nm. A smaller pigment peak located near 625 nm was present in all the spectra, exhibiting a slight drop near 5 m just as the 560 nm peak began to increase.

The early June (2005) phytoplankton absorption spectrum from OT was observed to flatten with depth down to 4 m, suggesting algal cells of increased packaging. A distinct pigment shoulder centered near 500 nm was observed at depths exceeding 5 m. This particular profile contained a dominant pigment signature at 560 nm which was not present at the surface,

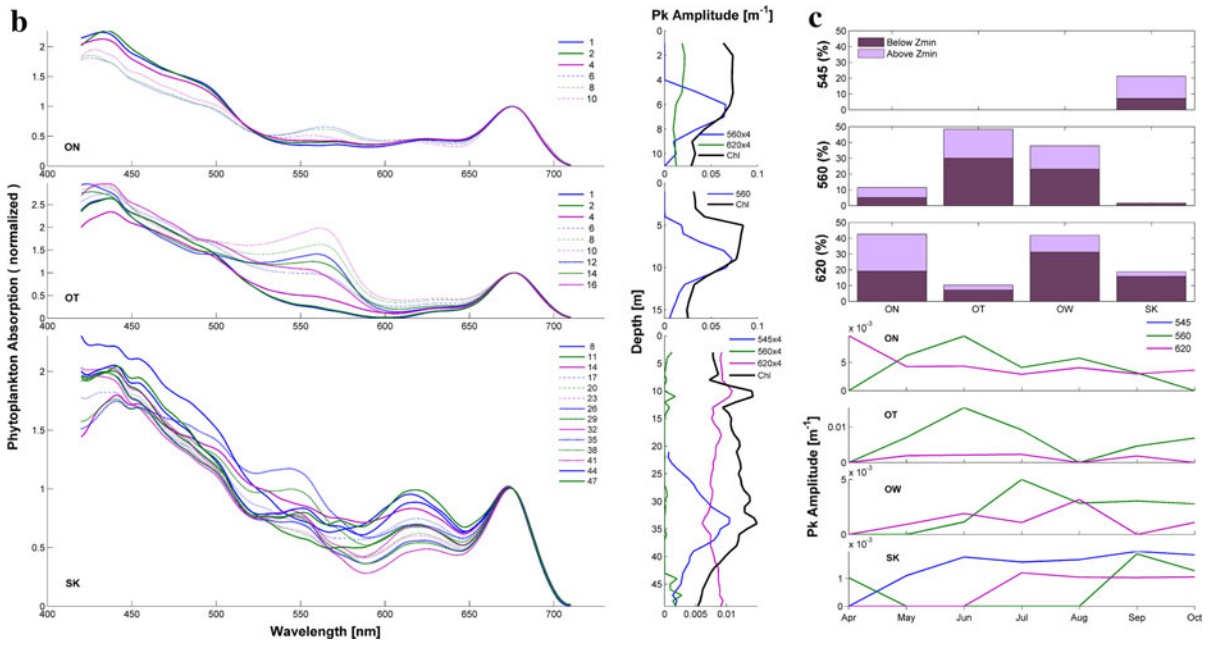

Fig. 4 continued

but became apparent at ca. 4 m and reached a maximum at 9 m coincident with a decline in [Chl *a*]; its line-height was nearly equal to that of Chl *a* (676 nm) at this depth and the peak persisted to the end of the profile (16 m).

The spectra from the SK sample were complex with many subtle absorption features. The most prominent were peaks at 545 nm below 20 m, the magnitude of which was 20% that of Chl *a* at 676 nm at 34 m coincident with [Chl *a*] reaching a maximum. The 560 nm peak found in the two previous examples was not present in SK spectra. However, a small peak centered near 575 nm was detected in select absorption spectra, many of which came from the deepest part of profiles (44–49 m). The most notable spectral feature, and present throughout the profile, was a peak that occurred between 620 and 625 nm. It reached a maximum near the surface in parallel with local peak in [Chl *a*], with an amplitude roughly 20% the height of Chl *a* at 676 nm. Note that, the amplitude minimum for this peak coincided with the maximum amplitude for 545 nm peak.

We analyzed the entire phytoplankton absorption dataset to determine the frequency of these prominent absorption peaks (i.e., 545, 560, and 625 nm, and 575 nm for SK), which we assume are not associated with chlorophylls or carotenoids (Fig. 4c). The 545 nm peak was detected only in SK and only 21% of the time, with one-third in depths greater than Z_{MIN}. The 560 nm absorption peak was most prominent in OT with an incident rate of 48% and mostly below Z_{MIN}. For OW, it was found in 38% of the spectra, 23% of which occurred below Z_{MIN}. In ON, we found it in only 11% of the spectra, half of it below Z_{MIN}. The 560 (575) nm peak was practically absent in SK (<2%). Overall, the presence of the 560 nm peak was highest in the two mesotrophic systems. The 620 nm pigment marker was observed ~42% of the time in both ON and OW, with 19 and 31% coming from below the euphotic zone, respectively. It was found in only 10% of OT spectra, three-quarters of which exceeded Z_{MIN}. In SK, this pigment was detected in 20% of the spectra and almost entirely from below Z_{MIN}. In terms of seasonal patterns, the 620 nm peak was not present in SK until July but nearly constant thereafter (Fig. 4c), varied little in ON or OT, while in OW considerable variation was observed reaching a maximum in August and a minimum in September; with respect to the 620 nm peak, patterns in all other pigments markers were relatively minor. However, the 560 nm peak did exhibit seasonal variation and was most pronounced in June in both ON and OT, in July for OW, and peaked in September for SK (but nearly absent during the summer months). With respect to the

545 nm pigment, it was found throughout the sampling season in SK, most consistently after the month of June.

Discussion

The in situ sensors used in this study provided valuable information about particle dynamics related to phytoplankton ecology in four dimictic temperate lake systems. The near continuous vertical hydrographic and optical measurements helped determine physical boundaries and surrogates to several biogeochemical parameters (respectively) in both the upper pelagic and profundal (dark) regions not achievable with more common sampling techniques.

Hydrographic variability and its effect on suspended particles

Thermal stratification is considered a key factor in the annual variability (and succession patterns) of phytoplankton biomass (Reynolds, 2002). In each of the four lakes sampled we found a strong association between stratification, and both Chl *a* and suspended particle concentrations in the upper water column. Factors affecting the formation and stability of the stratified regime are related to the depth of the lake relative to its surface area (e.g., Davis-Colley, 1988) and physical factors, such as wind exposure and light penetration (Wetzel, 2001). The three Finger Lakes (OT, OW, and SK), which are valley basins, all established stable epilimnions (in late summer) whose depth increased in proportion to the surface area of the lake (Table 1). For ON, the epilimnion was more varied and relatively shallow, often accompanied by a large metalimnion; the former condition is likely the result of strong light attenuation (e.g., $c_p(660)$; Table 2) limiting solar heating to the surface, whereas the latter is in part due to the surrounding metropolitan area providing little in the way of protection from wind exposure.

In each of the four lakes, once thermal gradients formed in late spring the vertical structure in algal biomass changed rapidly and was largely confined to the upper surface. Except for SK, this was partially explained by the close correlation between the base of metalimnion and the depth Z_{MIN}. If we ignore the effects of CDOM absorption, an increase in density across a temperature gradient causes the entrainment of small inorganic particles, as observed in several $c_p(660)$ and ξ profiles where the particle concentration increased relative to a decrease in particle size and independent of Chl *a* (e.g., 2005: October in OT or September in OW). The elevated mass of suspended material (plus CDOM) reduces PAR by increasing the vertical attenuation of light, thus limiting the warming of surface layer to a shallower depth which in turn increases the likelihood of finding Z_{MIN} near this boundary. A marked example occurred after a storm event in ON in July of 2006, where Z_{MIN} was located just above a twofold increase in particle concentration. Finally, the deepening of the mixed layer in late summer across each of the lakes caused a drop in [Chl *a*] with particle sizes generally decreasing; aside from dilution, contributing factors likely include a decline in nutrients, sinking of larger algal cells, reduction in absolute PAR, and possible grazing effects (Reynolds, 2006).

In medium-sized, well-stratified lakes, internal seiches can create currents near the bottom (or benthic) layer capable of re-suspending small particles (Kalff, 2002). Changes in both particle concentration and structure were observed near the bottom in both ON and OT. Specific to ON in September (2006), transitioning *away* from the bottom, the profiles exhibited a decrease in particle mass (decreasing $c_p(660)$) coupled to decreasing particle size (increasing ξ). This is consistent with particle re-suspension (Boss et al., 2001a). A similar event occurred in OT in June (2006) and August (2005). However, when the particle size decreases but particle mass increases approaching the bottom, as in June (2005) for OT, this is consistent with the existence of a nepheloid layer of aggregate detritial substances (Kalff, 2002); evidence from backscattering measurements suggests a small component of inorganic material was also present ($b_{bp}^{R} \sim 0.017$; not shown).

Temporal dynamics and vertical patterns of algal particles

The seasonal development of algal biomass in temperate lakes of moderate productivity often exhibit a pronounced spring bloom, followed by a summer decline, and a modest increase during fall turnover

(Wetzel, 2001). Except for ON which receives 20% of its inflow as effluent from a sewage treatment plant, the estimated concentration of total chlorophyll did not follow this pattern (Fig. 3). Although monthly variability was significant in the three remaining systems, any discernable Chl *a* maxima happened in July or August, with June and September having comparable levels depending on the system. A sizeable contribution to the total standing stock from depths below Z_{MIN} (1% PAR) was also observed, especially for ON, and in August for OT and OW. In addition and similar to other oligotrophic systems (Marshall & Peters, 1989), SK exhibited a delayed response (1–2 months) in Chl *a* buildup with little or no change approaching fall turnover.

Although the sample frequency was insufficient to fully resolve temporal variability, the high spatial resolution measurements were able to capture the vertical stratification of Chl *a*. In select years, at least three of the lake systems displayed coherent patterns of algal bloom formation and stratification. The distribution of phytoplankton in SK in 2006 exhibited vertical changes in chlorophyll levels that stratified into a threefold increase over several months, which was also apparent in both the beam attenuation and size parameter. The DCM in 2005 is worth mentioning not only because it is unique to oligotrophic systems (Reynolds, 2006), but the 5 m offset between particle beam attenuation and chlorophyll maxima indicates a decoupling of particle abundance from Chl *a*. This is likely the result of photoacclimation in the phytoplankton (e.g., Boss et al., 2007) and reinforces earlier studies cautioning the use of [Chl *a*] to infer biomass, especially oligotrophic systems (e.g., Cullen, 1982; Felip & Catalan, 2000; Fennel & Boss, 2003). Photoacclimation in the phytoplankton was also evident in OT at lower depths in both May and June, 2005, when the Chl *a* maxima de-coupled from particle concentration during the growth phase that led to the surface bloom in July. During this 3 months period the lack of modulation in the relative size of particulates across individual profiles suggests that the dominant algal populations were of similar size. In contrast to OT, the algal formation and subsequent bloom that occurred in ON (starting in June, 2005) saw a decline in both chlorophyll and particle mass near the center of the thermocline for prior to the rapid increase in surface chlorophyll in July. Here, the size parameter had markedly low surface values in July and August indicating a population of large phytoplankton (b_{bp}^{R} was ~0.008 at the surface; not shown).

In OW, chlorophyll concentration was more variable, especially in 2006, where a sizeable and unusual (given its size and no indicators showing up in the previous month) early surface bloom occurred in June. The subsequent decrease in $c_p(660)$ is consistent with a bloom die off and the increase in particle size at deeper depths in July suggests sinking algal cells. The modest bloom that followed in August was also unusual because of the relatively shallow Z_{MIN} of just 7 m. Here NAP was likely a contributing factor to the reduction in PAR (surface b_{bp}^{R} was ~0.02) and perhaps the result of a whiting event, which can follow an increase in photosynthesis and common in calcareous freshwater systems (Kalff, 2002). These distinct algal events in OW are in contrast to the other three lakes that did not exhibit such a rapid rise and fall in particle mass, suggesting the source of algal events were possibly allochthonous in origin.

Features in phytoplankton absorption spectra

Algae are characterized by the presence of photosynthetic pigments, including the primary light-harvesting pigment Chl *a*, accessory chlorophylls (mainly *b* and *c*), carotenoids, and biliproteins (Kirk, 2010). The chlorophyll-specific absorption spectra shown in Fig. 4a provides evidence of these accessory pigments (except chlorophyll *c*) by the location of the shoulder at 450 nm (chlorophyll *b*), the shoulder near 500 nm (carotenoids), and the broad subtle peak centered at 620 nm (e.g., biliproteins) (Rowan, 1989). Referred to as chromatic adaptation, phytoplankton cells increase the concentration of accessory pigments (per cell) relative to Chl *a* to augment photosynthesis in response to a reduction in absolute irradiance and the change in the spectrum of PAR with depth (Morel, 1978). Many accessory pigments are taxa specific (Rowan, 1989), and provide a means to detect phytoplankton groups using absorption spectra (e.g., Millie et al., 1997). In this study, we focused our attention on a small number of pigments which were relatively common in each lake (Fig. 4c), but more importantly their presence was more likely to be associated with stratification and a reduction in PAR (i.e., depths $\geq Z_{MIN}$). In contrast, many of the spectra not shown exhibited little in the way of distinct features in localized well-mixed

regions or during spring/fall turnover. Excluded from our analysis were carotenoids which are numerous and ubiquitous in algae (Rowan, 1989), but difficult to distinguish in absorption spectra. In addition, the line-height method used here was little affected by uncertainties in the partition model (methods) because the targeted peaks were readily observable (widely spaced and symmetric).

The spectra in Fig. 4b were not unique in this study but exemplary in illustrating chromatic adaptation; the response of which represents an assemblage of phytoplankton groups in the sample volume. The small but distinct shoulder near 480 nm in the ON sample is likely that of chlorophyll *b*, characteristic of green algae and common for the month of June in temperate lakes (Wetzel, 2001). It could also represent a non-photosynthetic (photoprotective) carotenoid pigment (e.g., β-carotene) as evidenced by a euphotic zone of roughly 7 m and its disappearance at deeper depths. The prominent peak centered at 560 nm is representative of the biliprotein, phycoerythrin (PE), a light-harvesting pigment common to blue–green algae. Photo-acclimation is made apparent by observing that PE was not present near the surface while its maxima coincided with Z_{MIN}, notably as the concentration of chlorophyll decreased. The ubiquitous but less discernable absorption peak near 620 nm is significant because the likely pigment, phycocyanin (PC), is also associated with cyanobacteria. Surprisingly, the occurrence of these pigments did not appear to be correlated (Fig. 4c). A possible explanation, offered by Falkowski & Raven (2007), is that PC pigment is the principle antenna (energy transfer) to PSII serving *all* cyanobacteria, while the production of PE has been shown to increase relative to PC when cells are exposed to green light (Glazer, 1977). This was indeed the case in the example spectra for ON (and OT) at depths approaching the base of the euphotic zone and could explain why PE was often found below Z_{MIN} during the months of maximum solar insolation for lakes having stable epilimnions (e.g., OT and OW; see Fig. 4c); the rarity of PE below Z_{MIN} in ON is likely due to a combination of a well-mixed layer (minimal photo-acclamation) and high light attenuation. Finally, the high incident rate of the PC peak at deeper depths (all lakes; Fig. 4c) could represent a dominant presence of cyanobacteria tolerant of low light levels with limited buoyancy control (i.e., species selection).

The spectra from OT are an example of how a PE-bearing population of algae changed chromatically in response to spectral changes in ambient light with depth. The pigment amplitude reached a maximum coincident with 1% PAR ($Z_{MIN} = 10$ m) and remained elevated in the 6 m that followed. Other profiles not shown from OT (June, 2005 and 2006) displayed similar chromatic changes as did select spectra from both OW and SK.

Discrete samples taken by local water authorities at sites close to the sampling buoy (<0.25 miles; sampling limited to upper 6 m) on the same date when the PE pigment peaks were observed were microscopically found to be dominated by algae of the genus *Dinobryon* (Chrysophyceae) and *Oscillatoria* (Cyanophyta) (Bryan Dristle, 2007, personal communication). *Oscillatoria* is a filamentous blue–green algae which can regulate its buoyancy and is tolerant of low light (Sukenik et al., 2010; also see Konopka et al., 1993). In addition, spectra in Fig. 4b shows evidence of a small shoulder at located at 460 nm, which is near the short wavelength peak of chlorophyll *c* (a principal light-harvesting pigment found in Chrysophyceae) consistent with the presence of *Dinobryon*.

While chlorophyll levels in SK were relatively low, typically on the order of 1 mg m^{-3}, spectral variation in the phytoplankton absorption coefficient was often considerable. While multiple pigments are readily apparent in Fig. 4b, the most prominent feature is centered at 620 nm and likely that of PC. Although present throughout the profile, it decreased gradually at deeper depths, coincident with an increase in a 545 nm absorption peak. To the best of our knowledge there is no distinct chromophore found at 545 nm, but Hoepffner & Sathyendranath (1991) using Gaussian decomposition techniques reported a pigment centered at 536 nm which they attributed to a mixture of carotenes and xanthophylls; both are light-harvesting carotenoids. Alternatively, the 545 nm pigment could represent a shift in the absorption peak of PE caused by pigment–protein complexes (Kirk, 2010), noting that the 560 peak was largely absent in SK (Fig. 4c). Given that PE and PC can exhibit a negative correlation (Prezelin & Boczar, 1986 and references therein), it's interesting that the 545 nm peak reached a maximum (~34 m) coincident with the PE peak reaching a

minimum. In either case, the strong correlation between the peaks at deeper depths and their presence throughout the sampling period (Fig. 4c) does support a relatively large and persistent standing stock of cyanobacteria. Furthermore, taxonomic studies by the water authorities conducted in the previous year (multiple stations; 60 m maximum depth at 3 m intervals) showed that SK was dominated throughout the season by *Cyclotella* (Bacillariophycae) and *Microcystis* (Cyanobacteria) (Dan Robbino, 2007, personal communication). The diatom *Cyclotella* contains chlorophyll *c*, which in addition to the primary peak at 460 nm also contains a small secondary peak near 570 nm; both are clearly evident in many of the individual spectrographs shown in Fig. 4b. Oddly, earlier studies showed that while *Cyclotella* was common in all these lakes, *Microcystis* was present only in ON and OW (Bloomfield, 1978). Subsequently however, *Microcystis* has now expanded to the entire Finger Lakes region (Boyer, 2007).

Conclusion

Modern in situ optical technology has the potential to change the current paradigm of monitoring lakes and further advance lake ecology in several ways by providing high resolution measurements that can be used to extract detailed information about the distribution of suspended particulates, and in particular, the spatial and temporal occurrence of phytoplankton. While adaptation strategies of phytoplankton, such as photoadaptation and depth regulation, are well documented (e.g., Cullen & MacIntyre, 1998), the profiles provided a lens into phytoplankton stratification unobtainable with conventional discrete sampling methods. By comparing vertical profiles of chlorophyll, the size parameter, and the presence of specific pigments, our sampling revealed that the phytoplankton variability in certain lakes (e.g., OT) was likely the result of changes in the dominance of a small number of algal species. While we acknowledge that our sampling lacked high temporal resolution and laboratory pigment analysis (e.g., HPLC), these observations are consistent with patterns documented in other temperate lakes (e.g., Meffert & Overbeck, 1985) and with microscopic analysis. In addition, the unique pigments peaks found many of the absorption spectra allowed us to infer cyanobacteria as a common algal type in each of the lakes studied. In situ profiling also permitted the estimation of the column integrated chlorophyll concentration, much of which was due to phytoplankton residing at or below the euphotic zone. As anthropogenic and climate change forcings increase (e.g., Nõges et al., 2010), increasing our current knowledge of the trophic capacity and condition of lakes can only improve our ability to recognize and address future impacts.

While this study was not supported by analysis of water samples for particle biogeochemical properties, we advocate both be done to provide validation and a better understanding of observed patterns. The data displayed here supports the use of autonomous platforms (e.g., profiling moorings with hydrographic and optical sensors) to resolve episodic (e.g., storm) events and provide the temporal and spatial scales necessary to quantify the variability in algal particles and optimize water sampling. This combined protocol can only enhance our understanding of freshwater biogeochemistry and biology, and aid in the management of lakes facing short and long-term forcings.

Acknowledgments We wish to thank the Upstate Freshwater Institute (UFI) for helping fund this research and for providing field instrumentation and assistance. UFI also performed the laboratory measurements. We are grateful to the staff at the School of Marine Sciences, University of Maine for technical and administrative support. The authors gratefully acknowledge valuable suggestions made by two anonymous reviewers. This contribution is No. 312 from the Upstate Freshwater Institute.

References

Babin, M., D. Stramski, G. M. Ferrari, H. Claustre, A. Bricaud, G. Obolensky & N. Hoepffner, 2003. Variations in the light absorption coefficients of phytoplankton, nonalgal particles, and dissolved organic matter in coastal waters around Europe. Journal of Geophysical Research 108(C7) 3211.1029/2001JC000882.

Babin, M., C. S. Roesler & J. J. Cullen (eds), 2008. Real-time coastal observing systems for marine ecosystem dynamics and harmful algal blooms: theory, instrumentation and modeling. UNESCO Publishing, Paris.

Belzile, C., W. Vincent, C. Howard-Williams, I. Hawes, M. R. James, M. Kumagai, & C. S. Roesler, 2004. Relationships between spectral optical properties and optically active substances in a clear oligotrophic lake. Water Resources Research 40: W12512.1029/2004WR003090.

Bloomfield, J. A., 1978. Lakes of New York State, Vol. I & II. Academic Press, New York.

Blough, N. V. & R. Del Vecchio, 2002. Chromophoric dissolved organic matter (DOM) in coastal environment. In Hansell,

D. A. & C. A. Carlson (eds), Biogeochemistry of marine dissolved matter. Academic Press, Boston.

Boss, E. & J. R. V. Zaneveld, 2003. The effect of bottom substrate on inherent optical properties: evidence of biogeochemical processes. Limnology and Oceanography 48: 346–354.

Boss, E., W. S. Pegau, W. D. Gardner, J. R. V. Zaneveld, A. H. Barnard, M. S. Twardowski, G. C. Chang & T. D. Dickey, 2001a. Spectral particulate attenuation and particle size distribution in the bottom boundary layer of a continental shelf. Journal of Geophysical Research 106: 9509–9516.

Boss, E. S., M. S. Twardowski & S. Herring, 2001b. Shape of the particulate beam attenuation spectrum and its inversion to obtain the shape of the particulate size distribution. Applied Optics 40: 4885–4893.

Boss, E., W. S. Pegau, M. Lee, M. Twardowski, E. Shybanov, G. Korotaev & F. Baratange, 2004. Particulate backscattering ratio at LEO 15 and its use to study particle composition and distribution. Journal of Geophysical Research 109: C0101410.1029/2002JC001514.

Boss, E. S., R. W. Collier, G. L. Larson, K. Fennel & W. S. Pegau, 2007. Measurements of spectral optical properties and their relation to biogeochemical variables and processes in Crater Lake, Crater Lake National Park, OR. Hydrobiologia 574: 149–159.

Boyer, G. L., 2007. Cyanobacterial toxins in New York and the lower Great Lakes ecosystems. In Hudnell, H. K. (ed.), Cyanobacterial Harmful Algal Blooms: State-of-the-Science and Research Needs. Springer, New York.

Bricaud, A. & D. Stramski, 1990. Spectral absorption coefficients of living phytoplankton and nonalgal biogenous matter: a comparison between the Peru upwelling area and the Sargasso Sea. Limnology and Oceanography 35: 562–582.

Bricaud, A., M. Babin, A. Morel & H. Claustre, 1995. Variability in the chlorophyll-specific absorption of natural phytoplankton: analysis and parameterization. Journal of Geophysical Research 100: 13321–13332.

Carder, K. L., R. G. Stewart, G. R. Harvey & P. B. Ortner, 1989. Marine humic and fulvic acids: their effects on remote sensing of ocean chlorophyll. Limnology and Oceanography 34: 68–81.

Ciotti, A. M., M. R. Lewis & J. J. Cullen, 2002. Assessment of the relationships between dominant cell size in natural phytoplankton communities and the spectral shape of the absorption coefficient. Limnology and Oceanography 47: 404–417.

Cleveland, J. S. & A. Weidemann, 1993. Quantifying absorption by aquatic particles: a multiple scattering correction for glass-fiber filters. Limnology and Oceanography 38: 1321–1327.

Coble, P. G., 2007. Marine optical biogeochemistry: the chemistry of ocean color. Chemical Reviews 107: 402–418.

Cullen, J. J., 1982. The deep chlorophyll maximum: comparing vertical profiles of chlorophyll *a*. Canadian Journal of Fisheries and Aquatic Sciences 39: 791–803.

Cullen, J. J. & J. G. MacIntyre, 1998. Behavior, physiology and the niche of depth-regulating phytoplankton. In Anderson, D. M., A. D. Cembella & G. M. Hallegraeff (eds), Physiological Ecology of Harmful Algal Blooms, NATO ASI Series Vol. G41.

Davis, R. F., C. C. Moore, J. R. V. Zaneveld & J. M. Napp, 1997. Reducing the effects of fouling on chlorophyll estimates derived from long-term deployments of optical instruments. Journal of Geophysical Research 102: 5851–5855.

Davis-Colley, R. J., 1988. Mixing depths in New Zealand lakes. New Zealand Journal of Marine and Freshwater Research 22: 517–527.

Dickey, T., M. Lewis & G. Chang, 2006. Optical oceanography: recent advances and future directions using global remote sensing and in situ observations. Reviews of Geophysics 44: RG1001.1029/2003RG000148.

Diehl, S., S. Berger, R. Ptacnik & A. Wild, 2002. Phytoplankton, light, and nutrients in a gradient of mixing depths: field experiments. Ecology 83: 399–411.

Duysens, L. N. M., 1956. The flattening of the absorption spectrum of suspensions as compared to solutions. Biochimica et Biophysica Acta 19: 1–12.

Edson, J. J. & R. C. Jones, 1988. Spatial, temporal, and storm runoff-related variations in phytoplankton community structure in a small, suburban reservoir. Hydrobiologia 169: 353–362.

Eisma, D., 1993. Suspended matter in the aquatic environment. Springer, New York.

Estapa, M. L., E. Boss, L. M. Mayer & C. S. Roesler, 2012. Role of iron and organic carbon in mass-specific light absorption by particulate matter from Louisiana coastal waters. Limnology and Oceanography 57: 97–112.

Falkowski, P. G. & J. A. Raven, 2007. Aquatic Photosynthesis, 2nd ed. Princeton University Press, Princeton.

Felip, M. & J. Catalan, 2000. The relationship between phytoplankton biovolume and chlorophyll in a deep oligotrophic lake: decoupling in their spatial and temporal maxima. Journal of Phytoplankton Research 22: 91–105.

Fennel, K. & E. Boss, 2003. Subsurface maxima of phytoplankton and chlorophyll: steady-state solutions from a simple model. Limnology and Oceanography 48: 1521–1534.

Ficek, D., S. Kaczmarek, J. Ston-Egiert, B. Wozniak, R. Majchrowski & J. Dera, 2004. Spectra of light absorption by phytoplankton pigments in the Baltic; conclusions to drawn from a Gaussian analysis of empirical data. Oceanologia 46: 533–555.

Fogg, G. E., 1991. The phytoplanktonic ways of life. New Phytologist 188: 191–232.

Gardner, W. D., I. D. Walsh & M. J. Richardson, 1993. Biophysical forcing on particle production and distribution during a spring bloom in the North Atlantic. Deep Sea Research II 40: 171–195.

Glazer, A. N., 1977. Structure and molecular organization of the photosynthetic assessor pigments of cyanobacteria and red algae. Molecular & Cellular Biochemistry 18: 125–140.

Hill, P. S., E. Boss, J. P. Newgard, B. A. Law & T. G. Milligan, 2011. Observations of the sensitivity of beam attenuation to particle size in a coastal bottom boundary layer. Journal of Geophysical Research 116: C02023.1029/2010JC006539.

Hoepffner, N. & S. Sathyendranath, 1991. Effect of pigment composition on absorption properties of phytoplankton. Marine Ecology Progress Series 73: 11–23.

Hoepffner, N. & S. Sathyendranath, 1993. Determine of the major groups of phytoplankton pigments from absorption spectra of total particulate matter. Journal of Geophysical Research 98(C12): 22789–22803.

Holdren, C., W. Jones & Taggart, 2001. Managing lakes and reservoirs. North American Lake Management Society and Terrene Institute, in cooperation with Office of Water, Assessment and Watershed Protection Division, US Environmental Protection Agency, Madison, WI.

Iqbal, M., 1983. An introduction to Solar Radiation. Academic Press, New York.

Johnsen, G. & E. Sakshaug, 2007. Biooptical characteristics of PSII and PSI in 33 species (13 pigment groups) of marine phytoplankton, and the relevance for pulse-amplitude-modulated and fast-repetition-rate fluorometry. Journal of Phycology 43: 1236–1251.

Kalenak, D. S., 2011. An optical study of four regional lakes in Upstate New York. PhD Thesis. State University of New York, College of Environmental Science and Forestry, New York.

Kalff, J., 2002. Limnology. Prentice Hall, Upper Saddle River.

Kirk, J. T. O., 2010. Light & Photosynthesis in Aquatic Ecosystems, 3rd ed. Cambridge University Press, Cambridge.

Konopka, A. E., A. R. Klemer, A. E. Walsby & B. W. Ibelings, 1993. Effects of macronutrients upon buoyancy regulation by metalimnetic *Oscillatoria agardhii* in Deming Lake, Minnesota. Journal of Plankton Research 15: 1019–1034.

Lampert, W. & U. Sommer, 2007. Limnoecology: The Ecology of Lakes and Streams. Oxford University Press, New York.

Lee, Z., A. Weidemann, J. Kindle, R. Arnone, K. L. Carder, & C. Davis, 2007. Euphotic zone depth: its derivation and implication to ocean-color remote sensing. Journal of Geophysical Research 122: C03009.1029/2006JC003802.

Marshall, C. T. & R. H. Peters, 1989. General patterns in the seasonal development of chlorophyll *a* for temperate lakes. Limnology and Oceanography 34: 856–867.

Marshall, C. T., A. Morin & R. H. Peters, 1988. Estimates of mean chlorophyll-a concentration: precision, accuracy, and sampling design. Journal of the American Water Resources Association 24: 1027–1034.

Meffert, M.-E. & J. Overbeck, 1985. Dynamics of chlorophyll and photosynthesis in natural phytoplankton associations: I. Seasonal and annual cycles of chlorophyll and phaeopigments, in relation to euphotic depth and their vertical distribution in small North German lakes. Archiv für Hydrobiologie Beihefte Ergebnisse der Limnologie 104: 219–234.

Millie, D. F., O. M. Schofield, G. J. Kirkpatrick, G. Johnsen, P. A. Tester & B. T. Vinyard, 1997. Detection of harmful algal blooms using photopigments and absorption signatures: a case study of the Florida red tide dinoflagellate, *Gymnodinium Breve*. Limnology and Oceanography 42: 1240–1251.

Mitchell, B. G., M. Kahru, J. Wieland & M. Stramska, 2003. Determination of spectral absorption coefficients of particles, dissolved material and phytoplankton for discrete samples. In Mueller, J. L., G. S. Fargion & C. R. McClain (eds), Ocean Optics Protocols for Satellite Ocean Color Sensor Validation, Revision 4, Vol. 4. NASA/TM-2003-21621, NASA Goddard Space Flight Center, Greenbelt, MD.

Moisan, J. R., T. A. H. Moisan & M. A. Linkswiler, 2011. An inverse modeling approach to estimating phytoplankton pigment concentrations from phytoplankton absorption spectra. Journal of Geophysical Research 116: C09018. 1029/2010JC006786.

Moore, C., A. Bernard, P. Fietzek, M. R. Lewis, H. M. Sosik, S. White & O. Zielinski, 2008. Optical tools for ocean monitoring and research. Ocean Science Discussions 5: 659–717.

Morel, A., 1974. Optical properties of pure water and pure sea water. In Jerlov, N. G. & E. S. Nielsen (eds), Optical Aspects of Oceanography. Academic Press, New York.

Morel, A., 1978. Available, usable, and stored radiant energy in relation to marine photosynthesis. Deep Sea Research 25: 673–688.

Mueller, J. L., 2003. In-water radiometric profile measurements and data analysis protocols. In Mueller, J. L., G. S. Fargion & C. R. McClain (eds), Ocean Optics Protocols for Satellite Ocean Color Sensor Validation, Revision 4, Vol. 3. NASA/TM-2003-21621, NASA Goddard Space Flight Center, Greenbelt, MD.

Nelson, J. R. & C. Y. Robertson, 1993. Detrital spectral absorption: laboratory studies of visible light effects on phytodetritus absorption, bacterial spectral signal, and comparison with field measurements. Journal of Marine Research 51: 181–207.

Nõges, P., R. Adrian, O. Anneville, L. Arvola, T. Blenckner, D. G. George, T. Jankowski, M. Järvinen, S. C. Maberly, J. Padisák, D. Straile, K. Teubner & G. Weyhenmeyer, 2010. The impact of variations in the climate on seasonal dynamics of phytoplankton. In George, D. G. (ed.), The Impact of Climate Change on European Lakes. Aquatic Ecology Series 4. Springer, Dordrecht: 253–274.

O'Donnell, D. M., S. W. Effler, C. M. Strait & G. A. Leshkevich, 2010. Optical characterizations and pursuit of optical closure for the western basin of Lake Erie through in situ measurements. Journal of Great Lakes Research 36: 736–746.

Oubelkheir, K., H. Claustre, A. Bricaud & M. Babin, 2007. Partitioning total spectral absorption in phytoplankton and colored detrital material contributions. Limnology and Oceanography: Methods 5: 384–395.

Perkins, M., S. W. Effler, C. Strait & L. Zhang, 2009. Light absorbing components in the Finger Lakes of New York. Fundamental and Applied Limnology 173: 305–320.

Pope, R. M. & E. S. Fry, 1997. Absorption spectrum (380–700 nm) of pure water. II. Integrating cavity measurements. Applied Optics 36: 8710–8723.

Preisendorfer, R. W., 1976. Hydrologic Optics, Volume V. Properties. U.S. Department of Commerce, National Oceanic and Atmospheric Administration, Environmental Research Laboratories, Honolulu.

Prezelin, B. B. & B. A. Boczar, 1986. Molecular basis of cell absorption and fluorescence in phytoplankton: potential applications to studies in optical oceanography. In Round, F. & D. Chapman (eds), Progress in Phycological Research. Biopress Ltd., Bristol.

Ptacnik, R., S. Diehl & S. Berger, 2003. Performance of sinking and nonsinking phytoplankton taxa in a gradient of mixing depths. Limnology and Oceanography 48: 1903–1912.

Reynolds, C. S., 2002. On the interannual variability in phytoplankton production in freshwater. In Williams, P. J. le B., D. N. Thomas & C. S. Reynolds (eds), Phytoplankton Productivity: Carbon Assimilation in Marine and Freshwater Ecosystems. Blackwell Science, Oxford.

Reynolds, C. S., 2006. Ecology of Phytoplankton. Cambridge University Press, Cambridge.

Roesler, C. S., 1998. Theoretical and experimental approaches to improve the accuracy of particulate absorption coefficients derived from the quantitative filter technique. Limnology and Oceanography 43: 1649–1660.

Roesler, C. S., M. J. Perry & K. L. Carder, 1989. Modeling in situ phytoplankton absorption from total absorption spectra in productive inland waters. Limnology and Oceanography 34: 1510–1523.

Rowan, K. S., 1989. Photosynthetic Pigments of Algae. Cambridge University Press, Cambridge.

Savitzky, A. & M. J. Golay, 1964. Smoothing and differentiation of data by simplified least squares procedures. Analytical Chemistry 36: 1627–1639.

Slade, W. H., E. Boss, G. Dall'Olmo, M. R. Langner, J. Loftin, M. J. Behrenfeld, C. Roesler & T. K. Westberry, 2010. Underway and moored methods for improving accuracy in measurement of spectral particulate absorption and attenuation. Journal of Atmospheric Oceanic Technology 27: 1733–1746.

Staehr, P. A., J. M. Testa, W. M. Kemp, J. J. Cole, K. Sand-Jensen & S. V. Smith, 2012. The metabolism of aquatic ecosystems: history, applications, and future challenges. Aquatic Sciences 74: 15–29.

Sukenik, A., T. Zohary & J. Padisak, 2010. Cyanoprokaryota and other prokaryota algae. In Likens, G. E. (ed.), Plankton of Inland Waters (A Derivative of Encyclopedia of Inland Waters). Academic Press, New York.

Sullivan, J. M., M. S. Twardowski, J. R. V. Zaneveld, C. M. Moore, A. H. Barnard, P. L. Donaghay & B. Rhoades, 2006. Hyperspectral temperature and salt dependences of absorption by water and heavy water in the 400–750 nm spectral range. Applied Optics 45: 5294–5309.

Twardowski, M. S., J. M. Sullivan, P. L. Donaghay & J. R. V. Zaneveld, 1999. Microscale quantification of the absorption by dissolved and particulate material in coastal waters with an ac-9. Journal of Atmospheric Oceanic Technology 16: 691–707.

Twardowski, M. S., E. Boss, J. B. Macdonald, W. C. Pegau, A. H. Barnard & J. R. V. Zaneveld, 2001. A model for estimating bulk refractive index from the optical backscattering ratio and the implications for understanding particle composition in case I and case waters. Journal of Geophysical Research 106(C7): 14129–14142.

Vanni, M. J., J. S. Andrews, W. H. Renwick, M. J. Gonzalez & S. J. Noble, 2006. Nutrient and light limitation of reservoir phytoplankton in relation to storm-mediated pulses in stream discharge. Archiv für Hydrobiologie 167: 421–455.

Voss, K. J., S. McLean, M. Lewis, C. Johnson, S. Flora, M. Feinholz, M. Yarbrough, C. Trees, M. Twardowski & D. Clark, 2010. An example crossover experiment for testing new vicarious calibration techniques for satellite ocean color radiometry. Journal of Atmospheric and Oceanic Technology 27: 1747–1759.

Watson, S. B., E. McCauley & J. A. Downing, 1997. Patterns in phytoplankton taxonomic composition across temperate lakes of differing nutrient status. Limnology and Oceanography 42: 487–495.

WET Labs Inc., 2008. Scattering Meter ECO BB–9 User's Guide. Philomath, OR [Available on internet at www.wetlabs.com/products/pub/eco/bb9j.pdf].

Wetzel, R. G., 2001. Limnology Lakes and River Ecosystems, 3rd ed. Academic Press, London.

Whitmire, S. B., W. S. Pegau, L. Karp-Boss, E. Boss & T. J. Cowles, 2010. Spectral backscattering properties of marine phytoplankton cultures. Optical Express 18: 15073–15093.

Zaneveld, J. R. V., J. Kitchen & C. Moore, 1994. Scattering error correction of reflecting tube absorption meter. In Jaffe, J. S. (ed,), Ocean Optics XII, International Society of Optical Engineering (SPIE Proceedings 2258): 44–55.

Zhang, Y., M. Liu, M. A. Van Dijk, G. Zhu, Z. Gong, Y. Li & B. Qin, 2009. Measured and numerically partitioned phytoplankton spectral absorption coefficients in inland waters. Journal of Plankton Research 31: 311–323.